Fish and Shellfish Immunology 87 (2019) 515–523

Contents lists available at ScienceDirect

Fish and Shellfish Immunology

journal homepage: www.elsevier.com/locate/fsi

Full length article

Dual RNA-seq reveals the effect of the *flgM* gene of *Pseudomonas plecoglossicida* on the immune response of *Epinephelus coioides*

Yujia Sun[a,b], Zhixia Zhuang[a], Xiaoru Wang[a], Huabin Huang[a], Qi Fu[a], Qingpi Yan[b,*]

[a] College of Environment and Public Health, Xiamen Huaxia University, Xiamen, Fujian 361024, China
[b] Fisheries College, Key Laboratory of Healthy Mariculture for the East China Sea, Ministry of Agriculture, Jimei University, Xiamen, Fujian 361021, China

ARTICLE INFO

Keywords:
Dual RNA-eq
Pseudomonas plecoglossicida
Epinephelus coioides
flgM
immune response

ABSTRACT

Pseudomonas plecoglossicida is an important and highly pathogenic bacterium for aquaculture and causes serious losses. The expression level of *flgM* was found to be significantly upregulated post-infection compared with *in vitro* results, which was confirmed by quantitative real-time PCR. RNAi significantly reduced the expression level of *flgM* mRNA of *P. plecoglossicida*. Compared with infection with the wild-type strain, infection with the *flgM*-RNAi strain resulted in a delay in death and a 75% reduction in the mortality of *Epinephelus coioides*, followed by alleviation of the symptoms in *E. coioides* spleen. Moreover, compared with infection with the wild-type strain, infection with the *flgM*-RNAi strain of *P. plecoglossicida* resulted in a significant change in the transcriptome of the spleens of infected *E. coioides* and *P. plecoglossicida*. KEGG analysis for *E. coioides* showed that genes of 17 immune pathways were most affected by *flgM*-RNAi of *P. plecoglossicida*. Among them, the expression of *mhc2*, *zap70*, *rhoh*, *tlr2*, *ca79a*, *hcst* and *cd32* in *E. coioides* spleen was predicted to be negatively related to *flgM* in *P. plecoglossicida* but positively related to genes involved in communication, metabolism and motility.

1. Introduction

All bacterial pathogens must adapt to sudden environmental changes in the host for survival [1]. Infection triggers a series of events that result in dynamic changes in the gene expression profiles in the pathogen and host [1]. Thus, simultaneous monitoring of the RNA expression profiles of the two interacting species during infection is important to obtain a comprehensive understanding of pathogenic mechanisms and the host's immune response [2]. As a sensitive tool for studying global gene expression of the host or pathogen in infection biology, RNA-seq has identified many important functional genes [3,4]. For a better understanding of the host-pathogen interaction, dual RNA-Seq was introduced to simultaneously profile host and pathogen transcriptomes for the first time in 2012 [3]. Recently, dual RNA-seq analyses were performed successfully in *Salmonella typhimurium* with HeLa cells [4] and *Streptococcus pneumonia* with lung epithelial cells for pathogen-host interactions [5].

Pseudomonas plecoglossicida is a gram-negative aerobic rod-shaped bacterium that is associated with epidemics of several marine fish such as *Oncorhynchus mykiss* and *Pseudosciaena crocea* [6]. In our previous work, the dual RNA-Seq transcriptome of *P. plecoglossicida*-infected *E. coioides* spleen at 1, 2, 3, and 4 days post-infection was sequenced and deposited in the NCBI Sequence Read Archive (SRA); the accession number is SRP115064. The comparative transcriptome analysis showed that *flgM* was significantly highly expressed at 2 days post infection.

The assembly of flagella is a precise and complex process in which at least 30 genes are coordinated, including *flgM* [7]. *flgM* is a flagellar biosynthesis anti-sigma factor that prevents flagellar class III promoter transcription by binding to σ^{28} [8]. σ^{28} is a flagellum-specific transcription factor that is transcribed from the flagellar class III promoter by RNA polymerase [9]. Until now, the function of *flgM* in pathogenicity has been very limited; meanwhile, no research has been reported about the roles of *flgM* during pathogen infection.

Considering the high mortality of *P. plecoglossicida* to economically cultured fish and the potential significant role of *flgM* in the virulence of *P. plecoglossicida*, *flgM* of *P. plecoglossicida* was silenced by RNAi. Then, the virulence to *E. coioides* was compared between the wild-type and *flgM*-RNAi strains of *P. plecoglossicida*. The spleens of *E. coioides* infected by the *flgM*-RNAi or wild-type strain of *P. plecoglossicida* were subjected to dual RNA-seq. The purpose of this paper is to uncover the immune response of *E. coioides* to the *flgM* gene of *P. plecoglossicida* by dual RNA-seq.

* Corresponding author.
E-mail address: yanqp@jmu.edu.cn (Q. Yan).

https://doi.org/10.1016/j.fsi.2019.01.041
Received 23 October 2018; Received in revised form 15 January 2019; Accepted 25 January 2019
Available online 29 January 2019

2. Materials and methods

2.1. Bacterial strains and culture conditions

P. plecoglossicida (NZBD9) was isolated from a naturally infected spleen of *P. crocea* [6]. The pathogen was grown in Luria-Bertani (LB) medium routinely at 18 °C with shaking at 220 rpm. *Escherichia coli* strain DH5α was acquired from TransGen Biotech (Beijing, China) and cultured in LB medium at 37 °C at 220 rpm. For the two strains, 10 μg/mL tetracycline was added to the medium when appropriate.

2.2. Construction of the P. plecoglossicida RNAi strain

The plasmid pCM130 was used for silencing target mRNA in *P. plecoglossicida* [10], as the plasmid was an effective carrier (named pCM130/tac) for expressing siRNA through the following design. After generating a specific oligonucleotide fragment by annealing a pair of synthetic shRNAs (synthetized by Generay Biotech Co., Ltd, Shanghai, China), the fragment was ligated between the *Bam*HI and *Sph*I (New England Biolabs, Ipswich, USA) restriction sites of the plasmid pCM130/tac.

The method of constructing the RNAi strain was carried out based on Darsigny et al. [11] and Choi and Schweizer [12]. Five siRNA sequences targeting 13–33 bp, 14–34 bp, 15–35 bp, 18–38 bp and 214–234 bp downstream from the translation initiation site of the *flgM* gene were designed and synthesized from Shanghai Generay Biotech Co., Ltd. (Shanghai, China; Supplementary Table 1). After linearizing pCM130/tac vectors with the restriction enzymes *Bsr*GI and *Nsi*I (New England Biolabs), the shRNAs were annealed and ligated to the linearized pCM130/tac vectors by T4 DNA ligase (New England Biolabs) in accordance with the manufacturer's recommendations. Then, recombinant pCM130/tac vectors were transformed into competent *E. coli* DH5α by heat shock and electroporated into competent *P. plecoglossicida* [13]. The tetracycline resistance marker was used for screening for stably silenced clones. After acquiring the five RNAi strains, these strains were cultured under the same conditions to extract RNA for reverse transcription. Finally, qRT-PCR was used for expression level detection of *flgM* to identify the best silencing site for subsequent experiments.

2.3. Epinephelus coioides infection experiments

All fish experiments were put into practice strictly under the recommendations of the 'National Institutes of Health Guide for the Care and Use of Laboratory Animals'. The animal protocols were carried out according to the Animal Ethics Committee of Jimei University (Acceptance NO JMULAC201159).

E. coioides infection was conducted by a modified version of protocols described earlier [6]. *E. coioides* in good health were obtained from Zhangzhou (Fujian, China) and were adaptively cultured at 18 °C under specific pathogen-free laboratory conditions for one week. Infection strains were cultured in LB medium to an OD600 of approximately 0.5 (24 h, 18 °C) and then washed and re-suspended in PBS at 18 °C.

Sixty size-matched *E. coioides* were injected intrapleurally with 10^3 colony-forming units of *P. plecoglossicida* (wild-type strain or the RNAi strains) per gram (cfu/g). *E. coioides* injected intrapleurally with PBS were used as a negative control. The water temperature was maintained at 18 °C during infection. The mortality of injected fish was recorded daily, and dead fish were cleared away in a timely manner. For the tissue distribution assays, several size-matched *E. coioides* were infected with the wild-type strain or the *flgM*-RNAi strain of *P. plecoglossicida*; then, three fish were sampled randomly at 24, 48, 72, 96 and 120 h post infection (hpi) for spleens, livers, blood, head kidneys and trunk kidneys.

For tissue dual RNA-seq assays, six size-matched *E. coioides* spleens infected with the wild-type strain or the *flgM*-RNAi strain of *P. plecoglossicida* were sampled at 48 hpi. Two spleens were mixed as one independent sample. Spleens of *E. coioides* infected with PBS were used as negative controls.

2.4. DNA extraction

DNA purification from spleens, livers, head kidneys and trunk kidneys was accomplished by an EasyPure Marine Animal Genomic DNA Kit (TransGen Biotech, Beijing, China) in accordance with the manufacturer's instructions. DNA purification from blood was accomplished by an EasyPure Blood Genomic DNA Kit (TransGen Biotech, Beijing, China).

2.5. RNA extraction

Total RNA was extracted by TRIzol reagent (Invitrogen, Carlsbad, CA, USA) in accordance with the manufacturer's instructions, while genomic DNA was digested using Turbo DNA-free DNase (Ambion, Austin, TX, USA). The quality of RNA was assessed by an Agilent 2100 Bioanalyzer (Agilent Technologies, Santa Clara, CA, USA), and rRNA was removed by a Ribo-Zero rRNA Removal Kit (Epicentre, Madison, WI, USA) in accordance with the manufacturer's instructions.

2.6. Quantitative real-time PCR (qRT-PCR)

qRT-PCR was performed by a QuantStudio 6 Flex (Life Technologies). All designed primer sequences are provided in Supplementary Table 2. The gene expression levels of *P. plecoglossicida* were normalized to that of 16S rDNA. The gene expression levels of *E. coioides* were normalized to that of *β-actin*. The $2^{-\Delta\Delta Ct}$ method was used to calculate the relative gene expression level.

2.7. cDNA library preparation and Illumina sequencing

The dual RNA-seq cDNA library was prepared using the TruSeq™ RNA Sample Preparation Kit (Illumina, San Diego, CA, USA). Briefly, the rRNA-depleted RNA samples were fragmented in fragmentation buffer, and cDNA synthesis was conducted using the SuperScript Double-Stranded cDNA Synthesis kit (Invitrogen, Carlsbad, CA, USA). After that, phosphorylation and poly (A) addition were carried out for end reparation, and the cDNA library was amplified by Phusion DNA polymerase (New England Biolabs). An Agilent 2100 Bioanalyzer (Agilent Technologies) was used to validate the library quality. Sequencing was carried out on an Illumina HiSeq4000 sequencing platform from Majorbio Biotech Co., Ltd. (Shanghai, China).

2.8. Processing and mapping of reads

The processing and quality control analysis of raw Illumina reads were performed by SeqPrep (https://github.com/jstjohn/SeqPrep) and Sickle (https://github.com/najoshi/sickle) with the default settings. Then, clean data were mapped to the NyZ12 strain genome of *P. plecoglossicida* (NCBI RefSeq accession numbers: NZ_ASJX00000000.1) by Bowtie2 [14]. Mapped reads were first classified as *P. plecoglossicida* reads, and leftover reads were used to obtain the *E. coioides* unigenes by de novo assembly.

2.9. de novo assembly and annotation of the E. coioides transcriptome

All clean reads, which were not mapped to the *P. plecoglossicida* genome, were treated as the reads pool. This reads pool was assembled into unigenes de novo using Trinity [15]. The clean unigenes were compared against four databases including STRING, SWISS-PROT, NCBI non-redundant (NR) protein and KEGG (Kyoto Encyclopedia of Genes and Genomes) databases by blastx to identify the proteins. Gene

Ontology (GO) annotations were conducted by the Blast2GO software (http://www.blast2go.com/b2ghome) [16]. Finally, KEGG was used for pathway analysis (http://www.genome.jp/kegg/) [17].

2.10. Analysis of differential gene expression

The measurement of differentially expressed genes was performed for libraries of *P. plecoglossicida* and *E. coioides*. Expression analyses of genes from the pathogen and host were based on annotations from NCBI (NZ_CP010359.1) and the reference transcriptome annotation for the *E. coioides* described above, respectively. After obtaining unique mapped read counts, the R package edgeR (version 3.10.2) [18] was used for testing differentially expressed genes, which met the following thresholds: $|\log2^{\text{fold change}}| \geq 1$ as well as false discovery rate (FDR) $^{<}0.05$.

2.11. KEGG enrichment analysis

KEGG pathway enrichment was carried out by KOBAS (KEGG Orthology-Based Annotation System) [19]. Fisher's exact test (adjusted p value ≤ 0.05) was used to test differentially expressed KEGG pathways. Genes in co-expression modules were enriched with Metascape (http://metascape.org) [20], and visualization was conducted with the "GOplot" package in R [21].

2.12. Weighted gene co-expression network analysis

R package weighted gene co-expression network analysis (WGCNA) [22] was used to predict the interaction between *P. plecoglossicida* and *E. coioides*. After calculating a pair-wise correlation matrix, the adjacency matrix was calculated by raising the correlation matrix according to a power β, which was selected in accordance with the scale-free topology criterion. Then, topological overlap was constructed. The cluster tree branch (the gene co-expression module) was constructed according to average linkage hierarchical clustering. Finally, module eigengenes were statistically classified, and highly similar modules were merged. The analytic results were visualized by Cytoscape software (http://www.cytoscape.org/).

2.13. Statistical analyses

All data are presented as the mean ± standard deviation (SD) from at least three sets of independent experiments. Data analysis was performed by SPSS 17.0 software (Chicago, IL, USA), while one-way analysis of variance was performed using Dunnett's test. p-Values < 0.05 were considered statistically significant.

2.14. Data access

The RNA sequencing read data were deposited in the GenBank SRA database under the accession numbers SRP115064 and SRP162281.

3. Result

3.1. The role of the flgM gene of P. plecoglossicida during infection

Fig. 1A shows the result of *flgM* gene expression of *P. plecoglossicida in vitro* and 48 h post-infection by qRT-PCR. The results showed that the expression level of the *flgM* gene was significantly higher at 48 hpi than *in vitro* (Fig. 1A), which was in accordance with the result of previous RNA-seq experiments.

Five shRNAs targeted on the sequence of the *flgM* gene were designed, and all of them significantly reduced the mRNA expression of the *flgM* gene with different efficiencies (Fig. 1B). The strain containing pCM130/tac-*flgM*-shRNA-18 (named the *flgM*-RNAi strain) exhibited the best silencing efficiency for the *flgM* gene and was selected for further studies. Although *flgM* was silenced, the growth of the *flgM*-RNAi strain was almost the same as that of the wild-type strain (Fig. 1C).

The spleens from the fish injected with the wild-type strain displayed typical symptoms (numerous white spots covered the spleen surface) at 96 hpi; however, no obvious white spots appeared on the spleen surface of *E. coioides* injected with the *flgM*-RNAi strain (Fig. 1D). Compared with their counterparts infected with the wild-type strain, the *E. coioides* infected with the *flgM*-RNAi strain exhibited a significant decrease in mortality and a significant delay in the time of death (Fig. 1E).

Fig. 1F shows the difference in the dynamic distribution of *P. plecoglossicida* between *E. coioides* infected with the *flgM*-RNAi strain and the wild-type strain. The percentage abundance of the *flgM*-RNAi strain compared to the wild-type strain varied over time and across different organs and increased over time post-infection, except in spleens. The percentage of the *flgM*-RNAi strain abundance compared to the wild-type strain abundance in the blood, head kidney and trunk kidney rose slightly at 72 hpi, and in the spleen and liver, the abundance declined from beginning to end, especially in the spleen.

3.2. Differentially expressed genes (DEGs) in the E. coioides transcriptome

The foundation of the RNA-seq approach is high-quality reads. The base distribution was balanced, while N% was in the reasonable range (Supplementary Fig. 1). The sequence data quality met the requirements of the subsequent analysis (Supplementary Fig. 2). The average distribution of the base error rate in the sequencing reads was less than 0.1% which was in the acceptable range (Supplementary Fig. 3). The reproducibility of the three biological duplicates was satisfactory (Supplementary Fig. 4). edgeR was used to calculate the gene expression profile; if the expression of a gene satisfied FDR < 0.05 and $|\log2FC| \geq 1$ at the same time, the gene was considered a differently expressed gene. In the present study, a total of 121,675 mRNAs were identified from the spleen infected by the *flgM*-RNAi strain. Compared with the mRNAs in the spleens infected by the wild-type strain, 24,563 mRNAs in the spleens infected by the *flgM*-RNAi strain were identified as significantly different in abundance, with 18,808 mRNAs downregulated and 5755 mRNAs upregulated (Fig. 2A); the expression level is shown in Fig. 2B. Some genes were selected from the transcriptome and confirmed by qRT-PCR (Supplementary Fig. 5).

According to the KEGG database, 16 immune-related KEGG pathways were enriched by all differentially expressed genes (DEGs). Compared with the genes in the spleen infected by the wild-type strain, a total of 258 DEGs were enriched in immune-related pathways, of which 159 were upregulated and 99 were downregulated. The chemokine signalling pathway was enriched and had 20 upregulated DEGs and 14 downregulated DEGs. The T cell receptor signalling pathway was enriched and had 18 upregulated DEGs and 8 downregulated DEGs. The Toll-like receptor signalling pathway was enriched and had 18 upregulated DEGs and 3 downregulated DEGs. The natural killer cell-mediated cytotoxicity pathway was enriched and had 12 upregulated DEGs and 6 downregulated DEGs. The Fc gamma R-mediated phagocytosis pathway was enriched and had 10 upregulated DEGs and 12 downregulated DEGs. The haematopoietic cell lineage pathway was enriched and had 10 upregulated DEGs and 5 downregulated 5 DEGs. The antigen processing and presentation pathway was enriched and had 10 upregulated DEGs and 1 downregulated DEGs. The leukocyte transendothelial migration pathway was enriched and had 8 upregulated DEGs and 12 downregulated DEGs. The NOD-like receptor signalling pathway was enriched and had 8 upregulated DEGs and 2 downregulated DEGs. The RIG-I-like receptor signalling pathway was enriched and had 8 upregulated DEGs and no downregulated DEGs. The intestinal immune network for IgA production pathway was enriched and had 8 upregulated DEGs and no downregulated DEGs. The platelet activation pathway was enriched and had 7 upregulated DEGs and 16

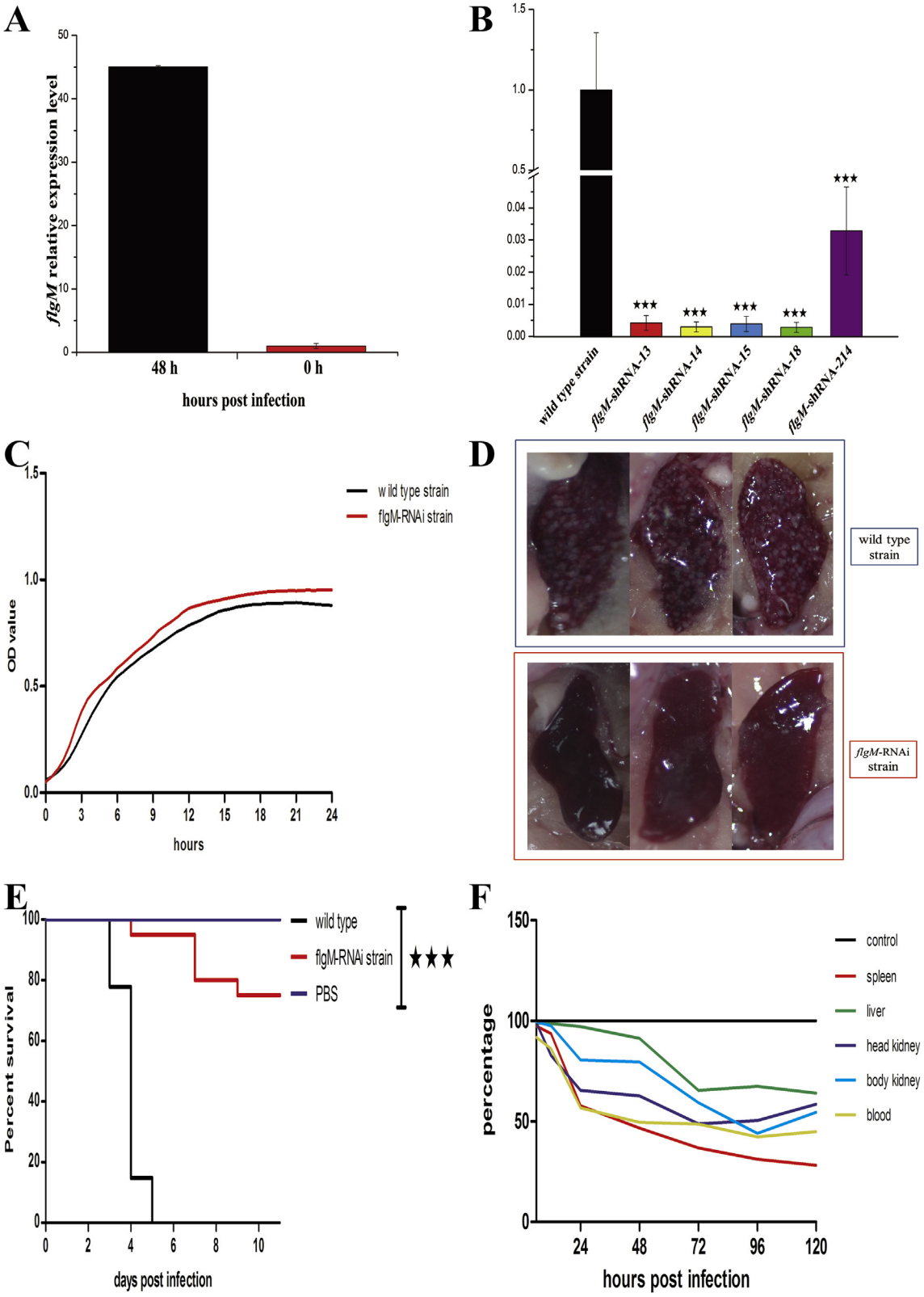

Fig. 1. The pathogenicity of *flgM* of *P. plecoglossicida* to *E. coioides* (A): The expression level of *flgM* mRNA at 48 hpi and *in vitro*. (B): The *flgM* mRNA levels of the 5 flgM-RNAi silencing strains. (C): Growth curve of the *flgM*-RNAi strain and wild-type strain. (D): Symptoms of *E. coioides* spleen infected by the wild-type or *flgM*-RNAi strain of *P. plecoglossicida*. (E): Survival curve of *E. coioides* infected by the wild-type or *flgM*-RNAi strain of *P. plecoglossicida*. ★★★$p \leq 0.001$. (F): Spatial and temporal distribution of the *flgM*-RNAi strain compared to the wild-type strain of *P. plecoglossicida*.

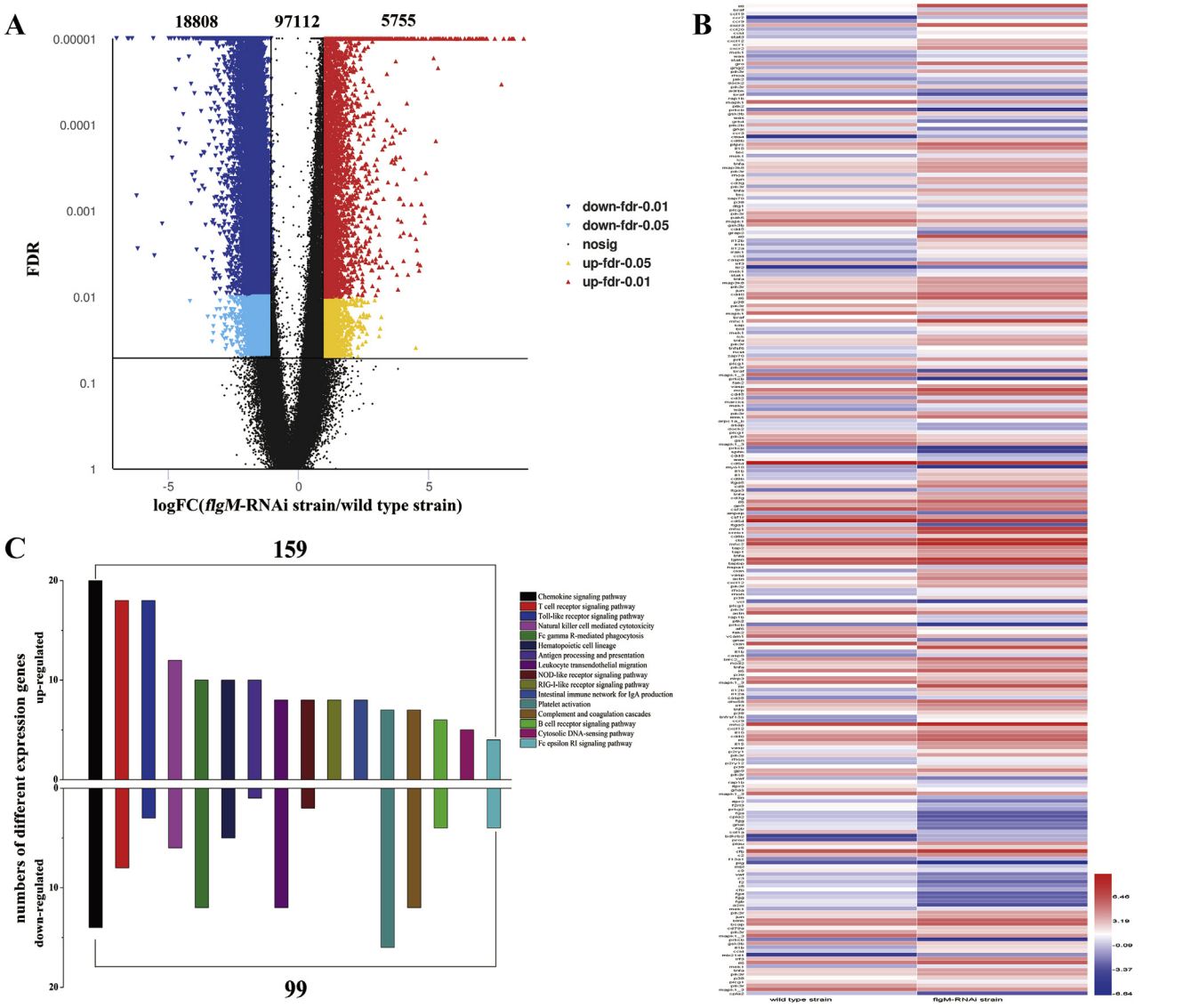

Fig. 2. Differentially expressed genes of spleens of *E. coioides* infected by *P. plecoglossicida* and KEGG analysis. (A): Volcano plot of all differentially expressed genes; the X-axis indicates the fold change values of spleens of *E. coioides* infected by the *flgM*-RNAi strain/spleens of *E. coioides* infected by the wild-type strain, the Y-axis indicates the statistical test value (FDR), and higher FDR values represent more significant differences. Each dot represents a gene: each red dot represents an upregulated gene; each blue dot represents a downregulated gene; and each black dot represents a non-significant difference gene. (B): Heat map of all differentially expressed genes. Values represent log2 fold changes. Colours are based on log-transformed FPKM mean values. Red and blue indicate increased and decreased expression, respectively. (C): The enrichment of immune-related KEGG pathways. (For interpretation of the references to colour in this figure legend, the reader is referred to the Web version of this article.)

downregulated DEGs. The complement and coagulation cascades pathway was enriched and had 7 upregulated DEGs and 12 downregulated DEGs. The B cell receptor signalling pathway was enriched and had 6 upregulated DEGs and 4 downregulated DEGs. The cytosolic DNA-sensing pathway was enriched and had 5 upregulated DEGs and no downregulated DEGs. The Fc epsilon RI signalling pathway was enriched and had 4 upregulated DEGs and 4 downregulated DEGs (Fig. 2C).

3.3. Differentially expressed genes (DEGs) of the P. plecoglossicida transcriptome

The foundation of the RNA-seq approach is high-quality reads. The base distribution was balanced, while N% was within the reasonable range (Supplementary Fig. 6). The sequence data quality met the requirements of the subsequent analysis (Supplementary Fig. 7). The average distribution of the base error rate in the sequencing reads was less than 0.1%, which is in the acceptable range (Supplementary Fig. 8). The reproducibility of the three biological duplicates was satisfactory (Supplementary Fig. 9). The gene expression profile was calculated by edgeR, and the changes in the expression level that met FDR < 0.05 and $|\log2FC| \geq 1$ were considered statistically significant differences. A total of 2322 mRNAs were identified from the spleens infected by the *flgM*-RNAi strain. Compared with the mRNAs in the spleens infected by the wild-type strain, 63 mRNAs in the spleens infected by the *flgM*-RNAi strain were identified as significantly different in abundance, with 13 mRNAs downregulated and 50 mRNAs upregulated (Fig. 3A); the expression levels are shown in Fig. 3B. Some genes were selected from the transcriptome and confirmed by qRT-PCR (Supplementary Fig. 10).

3.4. Prediction of the interaction between DEGs in P. plecoglossicida and immune pathway genes in E. coioides

The interaction between DEGs in *P. plecoglossicida* and immune

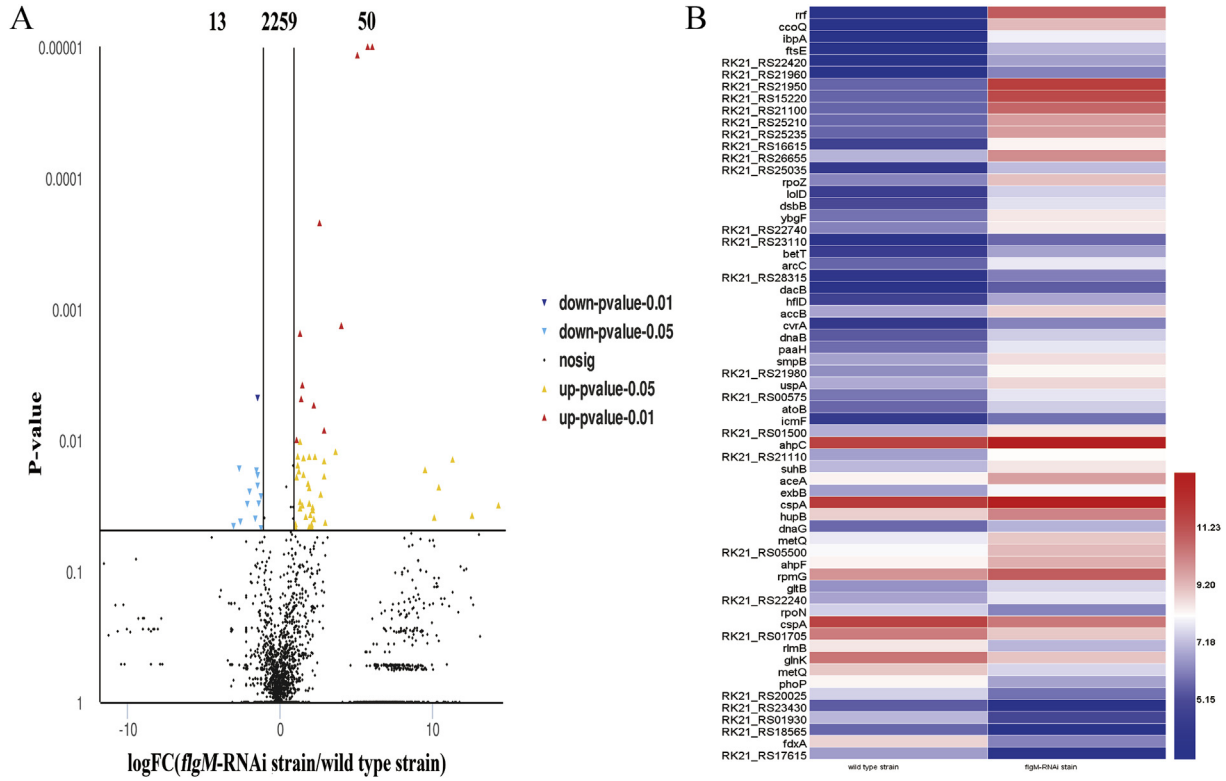

Fig. 3. *P. plecoglossicida* differentially expressed genes during infection of *E. coioides*. (A): Volcano plot of all differentially expressed genes; the X-axis indicates the fold change values of the *flgM*-RNAi strain/wild-type strain, the Y-axis indicates the statistical test value (FDR), and higher FDR values represent more significant differences. Each dot represents a gene: each red dot represents an upregulated gene; each blue dot represents a significantly downregulated gene; and each black dot represents a non-significant difference gene. (B): Heat map of all differentially expressed genes. Values represent log2 fold changes. Colours are based on log-transformed FPKM mean values. Red and blue indicate increased and decreased expression, respectively. (For interpretation of the references to colour in this figure legend, the reader is referred to the Web version of this article.)

pathway genes in *E. coioides* was predicted by the R package "WGCNA", with a power value of 18 (Supplementary Fig. 11 A, B) and a threshold of 0.6. Four modules were clustered: blue, brown, turquoise, and grey modules (Fig. 4A). *flgM* belonged to the brown module, and it had a negative correlation with *mhc2*, *zap70*, *rhoh*, *tlr2*, *cd79a*, *hcst*, *cd32*, *itga3*, *thfsf6*, and *arcC* and interacted with *mhc2*, *zap70*, *rhoh*, *tlr2*, *cd79a*, *hcst*, and *cd32* (Fig. 4B). These 7 immune genes were enriched in 8 pathways: *mhc2* was enriched in the antigen processing and presentation and intestinal immune network for IgA production pathways; *zap70* was enriched in the natural killer cell-mediated cytotoxicity and T cell receptor signalling pathways; *hcst* was enriched in the natural killer cell-mediated cytotoxicity pathway; *rhoh* was enriched in the leukocyte transendothelial migration pathway; *tlr2* was enriched in the Toll-like receptor signalling pathway; *cd79a* was enriched in the B cell receptor signalling pathway; and *cd32* was enriched in the Fc gamma R-mediated phagocytosis pathway (Fig. 4C).

3.5. The co-expression modules in E. coioides

The co-expressed DEGs in *E. coioides* were calculated by the R package "WGCNA", with a power value of 18, an experience value according to tutorials (Supplementary Fig. 11 C, D) and a threshold of

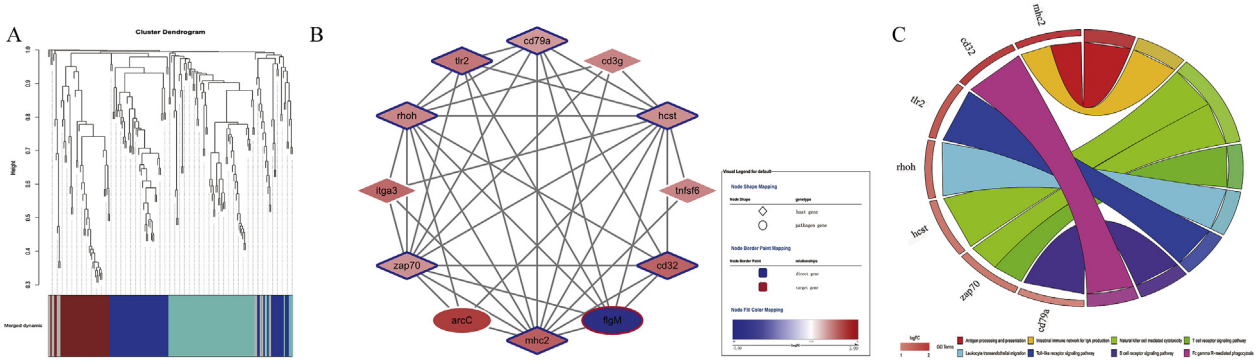

Fig. 4. Prediction of the gene regulatory network between all differentially expressed genes in *P. plecoglossicida* and immune pathway genes in *E. coioides*. (A): A hierarchical cluster tree conducted by WGCNA showed co-expression modules. Each leaf represents a gene, and each module corresponds to branches marked by different colours. (B): Gene co-expression network of the brown module. Circle nodes represent pathogen genes, while rhombi represent host genes. The red frame is *flgM*, and the blue frame indicates genes that interact with *flgM*. (C): Chordal graph of 7 immune genes to KEGG pathways. (For interpretation of the references to colour in this figure legend, the reader is referred to the Web version of this article.)

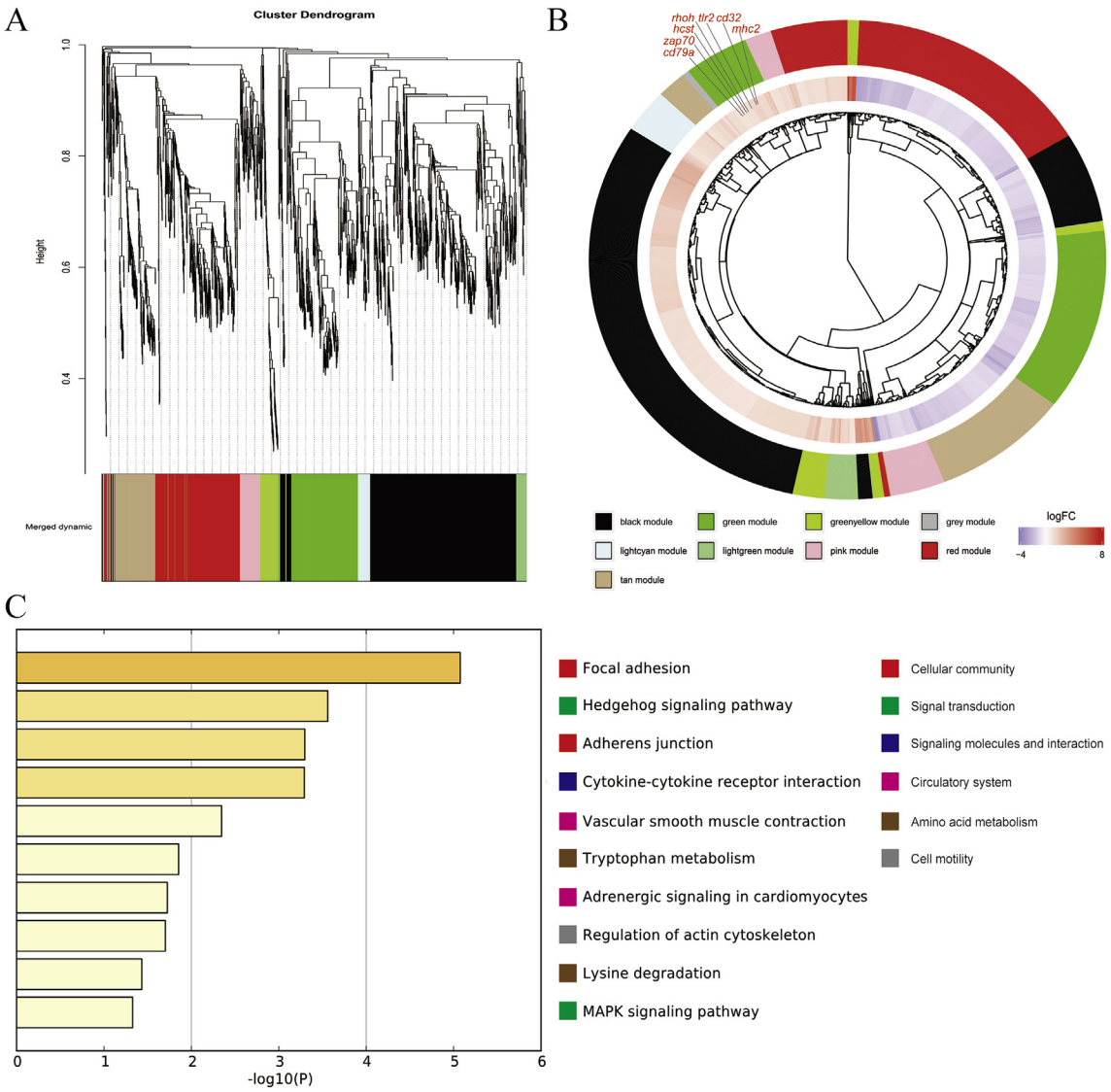

Fig. 5. Co-expressed genes with genes directly related to *flgM* in *E. coioides*. (A): A hierarchical cluster tree conducted by WGCNA showed all host differentially expressed gene co-expression modules. Each leaf represents a gene, and each module corresponds to branches marked by different colours. (B): Genes in each module. (C): KEGG pathways that were enriched with green module genes. (For interpretation of the references to colour in this figure legend, the reader is referred to the Web version of this article.)

0.7. Nine modules were clustered: black, green, green-yellow, grey, light cyan, light green, pink, red, and tan modules (Fig. 5A). The enrichment of genes is shown in Fig. 5B; *zap70*, *rhoh*, *tlr2*, *cd79a*, *hcst*, *cd32*, and *mhc2* belong to the green module. Genes belonging to the green module were enriched in KEGG pathways. Ranking by *p*-value, the top 10 KEGG pathways were the focal adhesion pathway, hedgehog signalling pathway, adherens junction pathway, cytokine-cytokine receptor interaction pathway, vascular smooth muscle contraction pathway, tryptophan metabolism pathway, adrenergic signalling in cardiomyocytes pathway, regulation of actin cytoskeleton pathway, lysine degradation pathway, and MAPK signalling pathway. The focal adhesion pathway and adherens junction pathway belong to cellular communication; the hedgehog signalling pathway and MAPK signalling pathway belong to signal transduction; the cytokine-cytokine receptor interaction pathway belongs to signalling molecules and interactions; the vascular smooth muscle contraction pathway and adrenergic signalling in cardiomyocytes pathway belong to the circulatory system; the tryptophan metabolism pathway and lysine degradation pathway belong to amino acid metabolism; and the regulation of the actin cytoskeleton pathway belongs to cell motility (Fig. 5C).

4. Discussion

Numerous genes are involved in the virulence regulation of pathogens by regulating toxicity and invasiveness [23]. Up to now, by knockdown or knockout technology, it has been verified that the ability of aquatic pathogenic bacteria to cause disease is regulated by different genes, such as *flgE* in *Aeromonas hydrophila* [24]; *oppABCDF, secA, secD, secF, yajC,* and *yidC* in *Vibrio alginolyticus* [25](13); and *sigX, L321_RS19110, L321_03626* and *L321_18122* in *P. plecoglossicida* [26–28]. However, no studies on the contribution of the *P. plecoglossicida flgM* gene to virulence have been reported.

Gene expression levels are regulated dynamically at different stages of pathogen infection of hosts [29]. The expression of *flgM* in *P. plecoglossicida* was significantly higher at 48 hpi than *in vitro*, which indicated that *flgM* might be involved in the virulence regulation of *P. plecoglossicida*. Compared with infection with the wild-type strain, infection with the *flgM*-RNAi strain caused the symptoms of *E. coioides* spleen to be alleviated and death was delayed, with a 75% reduction in *E. coioides* mortality. The results indicated that gene silencing of *flgM* resulted in a decrease in *P. plecoglossicida* virulence. Compared with

infection with the wild-type strain, infection with the *flgM*-RNAi strain caused the symptoms of *E. coioides* spleen to differ significantly; *E. coioides* spleen was the target organ of *P. plecoglossicida* [6], suggesting that *E. coioides* spleen is a good model to study the immune response of *E. coioides* to *P. plecoglossicida* infection.

It is well known that pathogen infection can cause great changes in both the host and pathogen transcriptomes [2,30]. Recently, it has been found that the change of a single virulence gene can also cause significant changes in the transcriptome [26,27]. In the present study, compared with the wild-type strain, the gene silencing of *flgM* in *P. plecoglossicida* resulted in a significant change in the transcriptomes of the infected spleen and invading *P. plecoglossicida*. There were 24,563 and 63 mRNAs differentially expressed in infected spleen and invading *P. plecoglossicida*, respectively. The results indicated that *flgM* of *P. plecoglossicida* had an important effect when invading *E. coioides*. The results of KEGG analysis of infected spleen showed that 16 immune-related pathways were significantly enriched, while the number of upregulated genes enriched in these pathways was 60 more than the number of downregulated genes, nearly 60% of the downregulated genes, in addition to the number of upregulated genes being over 10 in the chemokine signalling pathway, T cell receptor signalling pathway, Toll-like receptor signalling pathway and natural killer cell mediated cytotoxicity pathway. All of these genes belong to the innate immune pathway, except the T cell receptor signalling pathway, which belongs to the acquired immune pathway. This result suggested that innate immune pathways of *E. coioides* played an important role when *flgM*-RNAi strain infection occurred and that acquired immune pathways of *E. coioides* began to be activated at the same time. After pathogen invasion, leukocytes are delivered to the injury site and then trigger the immune response [31,32], including phagocytosis mediated by the Fc gamma receptor [33]. The Toll-like receptor signalling pathway is a well-known pathway for sensing pathogen invasion and activating the acquired immune system [34] via regulation of antigen processing and presentation [35]. The IgA generated is the first line of defence to pathogen invasion [36]. Natural killer cells circulate through the tissues, blood and lymphatics to identify and kill infecting microorganisms [37].

Through physical contact, organisms interact with other species constantly, which results in changes at the molecular level, such as in the transcriptome [38]. Faced with pathogen invasion, the host has to mobilize a series of immune mechanisms to resist [39]. In the present study, the results showed that 16 immune pathways changed when responding to *flgM*-RNAi strain invasion, and 7 immune genes in these immune pathways had a negative correlation with *flgM*, while these 7 immune genes were enriched in 8 immune pathways. When the host defends against pathogens, the immune pathways cooperate not only with each other but also with signal transduction and energy metabolism [40]. In the present study, the results showed that genes co-expressed with the 7 immune genes were enriched in 10 pathways, which belong to cellular communication, signal transduction, signalling molecules and interaction, circulatory system, amino acid metabolism, and cell motility. These pathway changes in the spleen of infected *E. coioides* were caused by the lack of *flgM* in *P. plecoglossicida*. The difference in these pathways in spleens infected with the *flgM*-RNAi strain indicated that *E. coioides* was more likely to kill the *flgM*-RNAi strain than the wild-type strain of *P. plecoglossicida.* These results also partly explain why the *flgM*-RNAi strain was less virulent and less abundant in *E. coioides*.

5. Conclusion

In conclusion, *flgM* was a pathogenic gene of *P. plecoglossicida* and contributed to the pathogenicity of *P. plecoglossicida* in *E. coioides.* Compared to infection with the wild-type strain, infection of *E. coioides* with the *flgM*-RNAi strain resulted in differences in the chemokine signalling pathway, T cell receptor signalling pathway, Toll-like receptor signalling pathway, natural killer cell-mediated cytotoxicity pathway, Fc gamma R-mediated phagocytosis pathway, haematopoietic cell lineage pathway, antigen processing and presentation pathway, leukocyte transendothelial migration pathway, NOD-like receptor signalling pathway, RIG-I-like receptor signalling pathway, intestinal immune network for IgA production pathway, platelet activation pathway, complement and coagulation cascades pathway, B cell receptor signalling pathway, cytosolic DNA-sensing pathway, Fc epsilon RI signalling pathway, focal adhesion pathway, hedgehog signalling pathway, adherens junction pathway, cytokine-cytokine receptor interaction pathway, vascular smooth muscle contraction pathway, tryptophan metabolism pathway, adrenergic signalling in cardiomyocytes pathway, regulation of actin cytoskeleton pathway, lysine degradation pathway, and MAPK signalling pathway.

Conflicts of interest

The authors declare that the research was conducted in the absence of any commercial or financial relationships that could be construed as a potential conflict of interest.

Acknowledgements

This work was supported by the Science and Technology Major / Special Project of Fujian Province under Contract No. 2016NZ0001-3 and the Natural Science Foundation of Fujian Province under Contract No. 2016J05080.

Appendix A. Supplementary data

Supplementary data to this article can be found online at https://doi.org/10.1016/j.fsi.2019.01.041.

References

[1] B. Baddal, A. Muzzi, S. Censini, R.A. Calogero, G. Torricelli, S. Guidotti, M. Soriani, Dual RNA-seq of nontypeable haemophilus influenzae and host cell transcriptomes reveals novel insights into host-pathogen cross talk, MBio 6 (6) (2015), https://doi.org/10.1128/mbio.00373-16 e01765-15.

[2] A.M. Nuss, M. Beckstette, M. Pimenova, C. Schmühl, W. Opitz, F. Pisano, P. Dersch, Tissue dual RNA-seq allows fast discovery of infection-specific functions and riboregulators shaping host–pathogen transcriptomes, Proc. Natl. Acad. Sci. Unit. States Am. 114 (5) (2017) E791–E800, https://doi.org/10.1073/pnas.1613405114.

[3] A.J. Westermann, S.A. Gorski, J. Vogel, Dual RNA-seq of pathogen and host, Nat. Rev. Microbiol. 10 (9) (2012) 618 https://doi.org/10.1038/nrmicro2852.

[4] A.J. Westermann, K.U. Förstner, F. Amman, L. Barquist, Y. Chao, L.N. Schulte, J. Vogel, Dual RNA-seq unveils noncoding RNA functions in host–pathogen interactions, Nature 529 (7587) (2016) 496, https://doi.org/10.1038/nature16547.

[5] R. Aprianto, J. Slager, S. Holsappel, J.W. Veening, Time-resolved dual RNA-seq reveals extensive rewiring of lung epithelial and pneumococcal transcriptomes during early infection, Genome Biol. 17 (1) (2016) 198, https://doi.org/10.1186/s13059-016-1054-5.

[6] L. Huang, W. Liu, Q. Jiang, Y. Zuo, Y. Su, L. Zhao, Q. Yan, Integration of transcriptomic and proteomic approaches reveals the temperature-dependent virulence of Pseudomonas plecoglossicida, Front. Cell. Infect. Microbiol. 8 (2018) 207, https://doi.org/10.3389/fcimb.2018.00207.

[7] S. Guo, I. Alshamy, K.T. Hughes, F.F. Chevance, Analysis of factors that affect FlgM-dependent type III secretion for protein purification with Salmonella Typhimurium, J. Bacteriol. 196 (13) (2014) 2333–2347, https://doi.org/10.1128/JB.01572-14 JB-01572.

[8] K. Ohnishi, K. Kutsukake, H. Suzuki, T. Lino, A novel transcriptional regulation mechanism in the flagellar regulon of Salmonella typhimurium: an anti-sigma factor inhibits the activity of the flagellum-specific Sigma factor, σF, Mol. Microbiol. 6 (21) (1992) 3149–3157, https://doi.org/10.1111/j.1365-2958.1992.tb01771.x.

[9] K. Ohnishi, K. Kutsukake, H. Suzuki, T. Iino, Gene fliA encodes an alternative sigma factor specific for flagellar operons in Salmonella typhimurium, Mol. Gen. Genet. MGG 221 (2) (1990) 139–147 https://doi.org/10.1007/BF00261713.

[10] Y.Z. Gao, H. Liu, H.J. Chao, N.Y. Zhou, Constitutive expression of nag-like dioxygenase gene through an internal promoter in the 2-chloronitrobenzene catabolic gene cluster of Pseudomonas stutzeri ZWLR2-1, Appl. Environ. Microbiol. 82 (12) (2016) 3461–3470, https://doi.org/10.1128/AEM.00197-16 AEM-00197.

[11] M. Darsigny, J.P. Babeu, E.G. Seidman, F.P. Gendron, E. Levy, J. Carrier, F. Boudreau, Hepatocyte nuclear factor-4α promotes gut neoplasia in mice and protects against the production of reactive oxygen species, Cancer Res. 70 (22) (2010) 9423–9433, https://doi.org/10.1158/0008-5472 0008-5472.

[12] K.H. Choi, H.P. Schweizer, mini-Tn7 insertion in bacteria with single attTn7 sites: example Pseudomonas aeruginosa, Nat. Protoc. 1 (1) (2006) 153, https://doi.org/10.1038/nprot.2006.24.
[13] G. Luo, L. Huang, Y. Su, Y. Qin, X. Xu, L. Zhao, Q. Yan, flrA, flrB and flrC regulate adhesion by controlling the expression of critical virulence genes in Vibrio alginolyticus, Emerg. Microb. Infect. 5 (8) (2016) e85, https://doi.org/10.1038/emi.2016.82.
[14] B. Langmead, S.L. Salzberg, Fast gapped-read alignment with Bowtie 2, Nat. Methods 9 (4) (2012) 357, https://doi.org/10.1038/NMETH.1923.
[15] I. Estensoro, G. Pérez-Cordón, A. Sitjà-Bobadilla, M.C. Piazzon, Bromodeoxyuridine DNA labelling reveals host and parasite proliferation in a fish-myxozoan model, J. Fish. Dis. 41 (4) (2018) 651–662, https://doi.org/10.1111/jfd.12765.
[16] A. Conesa, S. Götz, J.M. García-Gómez, J. Terol, M. Talón, M. Robles, Blast2GO: a universal tool for annotation, visualization and analysis in functional genomics research, Bioinformatics 21 (18) (2005) 3674–3676, https://doi.org/10.1093/bioinformatics/bti610.
[17] M. Kanehisa, S. Goto, KEGG: kyoto encyclopedia of genes and genomes, Nucleic Acids Res. 28 (1) (2000) 27–30 https://doi.org/10.1093/nar/28.1.27.
[18] M.D. Robinson, D.J. McCarthy, G.K. Smyth, edgeR: a Bioconductor package for differential expression analysis of digital gene expression data, Bioinformatics 26 (1) (2010) 139–140, https://doi.org/10.1093/bioinformatics/btp616.
[19] C. Xie, X. Mao, J. Huang, Y. Ding, J. Wu, S. Dong, L. Wei, KOBAS 2.0: a web server for annotation and identification of enriched pathways and diseases, Nucleic Acids Res. 39 (suppl_2) (2011) W316–W322, https://doi.org/10.1093/nar/gkr483.
[20] S. Tripathi, M.O. Pohl, Y. Zhou, A. Rodriguez-Frandsen, G. Wang, D.A. Stein, E. Yángüez, Meta-and orthogonal integration of influenza "OMICs" data defines a role for UBR4 in virus budding, Cell Host Microbe 18 (6) (2015) 723–735, https://doi.org/10.1016/j.chom.2015.11.002.
[21] W. Walter, F. Sánchez-Cabo, M. Ricote, GOplot: an R package for visually combining expression data with functional analysis, Bioinformatics 31 (17) (2015) 2912–2914, https://doi.org/10.1093/bioinformatics/btv300.
[22] P. Langfelder, S. Horvath, WGCNA: an R package for weighted correlation network analysis, BMC Bioinformatics 9 (1) (2008) 559, https://doi.org/10.1186/1471-2105-9-559.
[23] A. Beceiro, M. Tomás, G. Bou, Antimicrobial resistance and virulence: a successful or deleterious association in the bacterial world? Clin. Microbiol. Rev. 26 (2) (2013) 185–230, https://doi.org/10.1128/CMR.00059-12.
[24] Y. Qin, G. Lin, W. Chen, X. Xu, Q. Yan, Flagellar motility is necessary for *Aeromonas hydrophila* adhesion, Microb. Pathog. 98 (2016) 160–166, https://doi.org/10.1016/j.micpath.2016.07.006.
[25] W. Liu, L. Huang, Y. Su, Y. Qin, L. Zhao, Q. Yan, Contributions of the oligopeptide permeases in multistep of *Vibrio alginolyticus* pathogenesis, MicrobiologyOpen 6 (5) (2017), https://doi.org/10.1002/mbo3.511 e00511.
[26] Y. Sun, G. Luo, L. Zhao, Y. Qin, L. Huang, Y. Su, Q. Yan, Integration of rnai and rna-seq reveals the immune responses of *Epinephelus coioides* to *sigX* gene of *Pseudomonas plecoglossicida*, Front. Immunol. 9 (2018) 1624, https://doi.org/10.3389/fimmu.2018.01624.
[27] B. Zhang, G. Luo, L. Zhao, L. Huang, Y. Qin, Y. Su, Q. Yan, Integration of RNAi and RNA-seq uncovers the immune responses of *Epinephelus coioides* to L321_RS19110 gene of *Pseudomonas plecoglossicida*, Fish Shellfish Immunol. 81 (2018) 121–129, https://doi.org/10.1016/j.fsi.2018.06.051.
[28] L. Huang, Y. Zuo, Q. Jiang, Y. Su, Y. Qin, Q. Yan, A metabolomic investigation into the temperature-dependent virulence of *Pseudomonas plecoglossicida* from large yellow croaker (Pseudosciaena crocea), J. Fish. Dis. (2019), https://doi.org/10.1111/jfd.12957.
[29] A. Hey, M.S. Li, M.J. Hudson, P.R. Langford, J.S. Kroll, Transcriptional profiling of Neisseria meningitidis interacting with human epithelial cells in a long-term in vitro colonisation model, Infect. Immun. 81 (11) (2013) 4149–4159, https://doi.org/10.1128/IAI.00397-13 IAI-00397.
[30] L. Huang, W. Liu, Q. Jiang, Y. Zuo, Y. Su, L. Zhao, Y. Qin, Q. Yan, Integration of transcriptomic and proteomic approaches reveals the temperature-dependent virulence of *Pseudomonas plecoglossicida*, Front. Cell. Infect. Microbiol. 8 (2018) 207, https://doi.org/10.3389/fcimb.2018.00207.
[31] A.M. Wohlleben, F. Franke, M. Hamley, J. Kurtz, J.P. Scharsack, Early stages of infection of three-spined stickleback (Gasterosteus aculeatus) with the cestode Schistocephalus solidus, J. Fish. Dis. 41 (11) (2018) 1701–1708, https://doi.org/10.1111/jfd.12876.
[32] W.A. Muller, Mechanisms of leukocyte transendothelial migration, Annu. Rev. Pathol. 6 (2011) 323–344, https://doi.org/10.1146/annurev-pathol-011110-130224.
[33] E. García-García, C. Rosales, Signal transduction during Fc receptor-mediated phagocytosis, J. Leukoc. Biol. 72 (6) (2002) 1092–1108 https://doi.org/10.1189/jlb.72.6.1092.
[34] S. Akira, K. Takeda, Toll-like receptor signalling, Nat. Rev. Immunol. 4 (7) (2004) 499, https://doi.org/10.1038/nri1391.
[35] J.M. Vyas, A.G. Van der Veen, H.L. Ploegh, The known unknowns of antigen processing and presentation, Nat. Rev. Immunol. 8 (8) (2008) 607, https://doi.org/10.1038/nri2368.
[36] B. Mi, G. Liu, W. Zhou, H. Lv, K. Zha, Y. Liu, J. Liu, Bioinformatics analysis of fibroblasts exposed to TGF-β at the early proliferation phase of wound repair, Mol. Med. Rep. 16 (6) (2017) 8146–8154, https://doi.org/10.3892/mmr.2017.7619.
[37] L.L. Lanier, Up on the tightrope: natural killer cell activation and inhibition, Nat. Immunol. 9 (5) (2008) 495, https://doi.org/10.1038/ni1581.
[38] S. Schulze, J. Schleicher, R. Guthke, J. Linde, How to predict molecular interactions between species? Front. Microbiol. 7 (2016) 442, https://doi.org/10.3389/fmicb.2016.00442.
[39] J. Parkin, B. Cohen, An overview of the immune system, Lancet 357 (9270) (2001) 1777–1789, https://doi.org/10.1016/S0140-6736(00)04904-7.
[40] K. Ganeshan, A. Chawla, Metabolic regulation of immune responses, Annu. Rev. Immunol. 32 (2014) 609–634, https://doi.org/10.1146/annurev-immunol-032713-120236.